A spectral-timing approach to the study of AGN outflows

de Jesus Silva, C.V.

Publication date
2018
Document Version
Other version
License
Other

1 Introduction

1.1 Active Galactic Nuclei

Active galactic nuclei (AGN) are incredibly luminous. The luminosities in the nuclei of active galaxies can exceed the total luminosity of the host galaxy by several orders of magnitude ($L_{\mathrm{bol_{AGN}}} \sim 10^{40} - 10^{47}$ergs s^{-1}). The persistent, broadband, emission is powered by accretion of surrounding material onto a supermassive black hole ($10^6 - 10^9 \mathrm{M}_\odot$; Rees 1984). Infall of matter in the vicinity of a black hole is also associated with outflow events. Powerful outflows from AGN can strongly influence its host galaxy, or even the intracluster medium, a phenomenon known as AGN feedback (Fabian 2012; King & Pounds 2015). Assessing the nature and characteristics of the outflows are hence crucial to the understanding of large-scale structure formation and evolution in the Universe.

1.1.1 Spectral energy distribution

Extensive observations throughout the past decades, across the whole electromagnetic spectrum, allowed a canonical picture of these objects to be inferred (see Padovani et al. 2017, for a recent review). Due to the extreme luminosities and rapid variability (hence compact volumes) associated with the emission from the central regions of active galaxies, it soon became clear that AGN must be powered by a process more efficient than stellar processes (e.g. Fabian 1979). Accretion onto a central supermassive black hole was first proposed in the 60s (Salpeter 1964; Zel'dovich & Novikov 1964; see also Rees 1984) and is currently widely accepted as the likely mechanism responsible for powering AGN.

The standard AGN paradigm (Antonucci 1993; Urry & Padovani 1995) can be described as follows and is schematicaly represented in Fig. 1.1. A simplified diagram

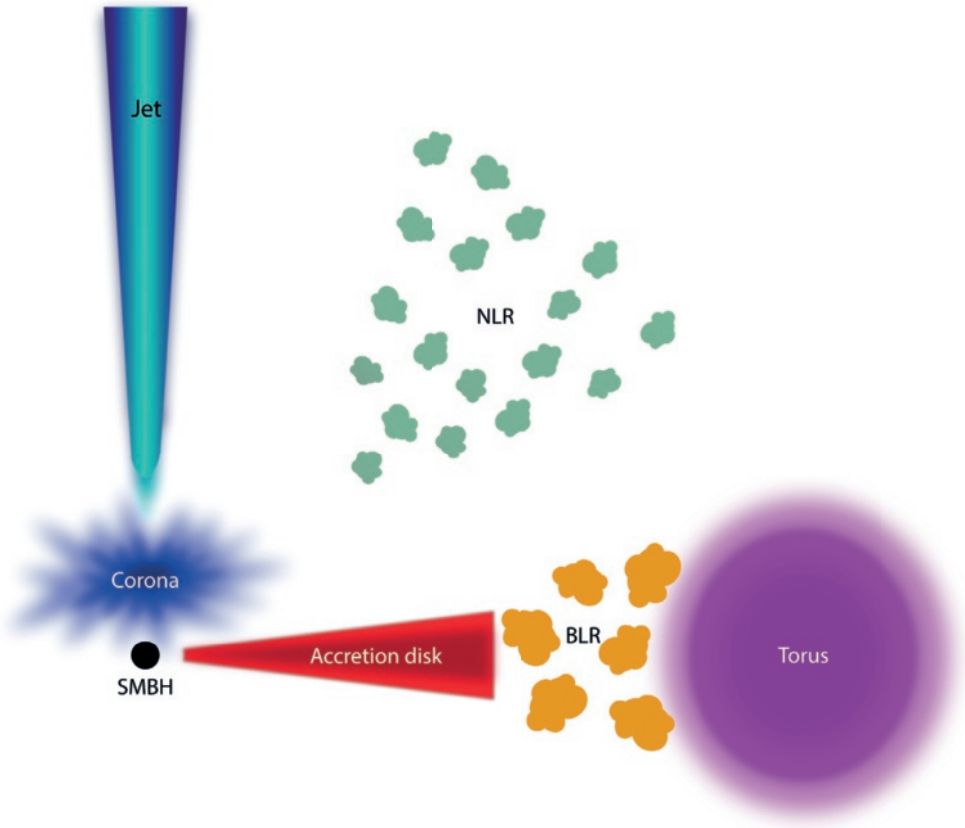

Figure 1.1: Schematic view of the unified model of AGN.

of the corresponding spectral energy distribution (SED) is shown in Fig. 1.2. The gas in the vicinity of the black hole forms an accretion disk, due to the angular momentum that is carried by the in-falling matter. Viscous forces in the disk are then responsible for dissipating energy and carrying angular momentum outwards, thus driving the gas in. Radiation from the accretion disk produces a thermal blackbody emission profile which peaks in the optical/UV (dashed red line in Fig. 1.2), as expected from a standard optically thick, geometrically thin disk (Shakura & Sunyaev 1973). Most of the X-ray emission observed from AGN is well modelled by a hard power-law component with a cut-off at high energies (see dashed blue line in Fig. 1.2). This non-thermal component is assumed to originate in a hot, optically thin medium, generally referred to as the 'corona', through the up-scattering of disk photons by Comptonization (Haardt & Maraschi 1993). While the geometry of the corona is not fully understood, variability arguments suggest it to be very compact (see more

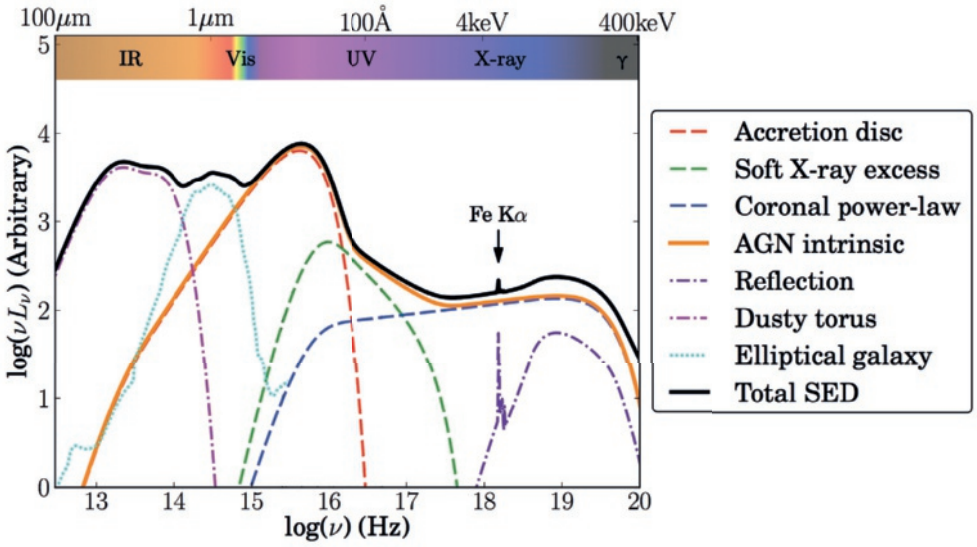

Figure 1.2: Simplified schematic diagram of an AGN SED highlighting the contribution of the different emission mechanisms. Adapted from Collinson et al. (2017).

in Section 1.1.2). Reprocessing of the hot coronal emission in the disk results in observable reflection signatures, characteristic of a reflection spectrum (Lightman & White 1988), particularly in the hard X-rays through the reflection hump, see dashed-dotted purple line in Fig. 1.2 (George & Fabian 1991; Done 2010). An additional signature of the reflection spectrum is the presence of a fluorescent Fe K-α emission line at $\sim 6.4\,\mathrm{keV}$. Reflection from the inner disc may further contribute to the observed 'soft excess' (Crummy et al. 2006; Fabian et al. 2009), although this component can also be attributed to partially ionized absorption (Gierliński & Done 2004) or to inverse Compton processes within the disk (Done et al. 2012).

In addition to the continuum emission from the accretion disk, the optical/UV spectrum of AGN is populated by emission lines. The emission lines arise due to ionization of the surrounding material by the central source. In particular, these emission lines are thought to originate from two distinct gaseous environments, the broad-line region (BLR) and the narrow-line region (NLR) (see Fig. 1.1). The BLR, formed by large column density clouds, is responsible for the emission of lines whose profiles are broadened by several thousand $\mathrm{km\,s^{-1}}$. These high-density clouds are located at $\leq$ 1pc from the central engine and their kinematics are dominated by virialized motions around the central black hole (Gaskell 1988). Characterization of the BLR through reverberation mapping (see Section 1.1.2, for details) allows tight constraints to be placed on the masses of the central black holes, as well as providing new insights on the geometry of this region. Broad emission lines have also been

detected in high-resolution X-ray spectra, whose widths and fluxes are consistent with a BLR origin (e.g Costantini et al. 2016).

Narrow emission lines, often observed in the optical and the UV, are instead believed to be produced by clouds located further from the source (up to ~ 3 kpc, Bennert et al. 2006) with widths of the order of several hundreds of $\mathrm{km\,s^{-1}}$. The presence of narrow forbidden lines implies a low density for the clouds in the NLR. While narrow emission lines are widely detected in the spectra of active galaxies, only a subset of AGN show the presence of broad lines. Polarization studies revealed that some of the AGN apparently lacking such broad-lines were in fact obscured, and the lines resultant from the turbulent gas in the broad-line region could be detected when seen in polarised light (Antonucci & Miller 1985). Such observations led to the proposal of the AGN unification model (Antonucci 1993; Urry & Padovani 1995, and references therein), where the differences in the observations of Type – 1 and Type – 2 AGN are attributed to the object's orientation with respect to the observer's line-of-sight. The key element in the paradigm is the presence of an obscuring dusty torus, which sits in the equatorial plane (see Fig. 1.1), at about 1 pc, or less, from the central source. When the line-of-sight intersects the torus, only narrow lines are detected and a Type – 2 AGN is observed. On the contrary, Type – 1 AGN, showing the presence of both narrow and broad emission lines, are observed when the line-of-sight is not at the equatorial plane, hence not intersecting the obscuring torus. Despite its simplicity and drawbacks (see Netzer 2015, for a recent review), this model quite successfully explains observations of a wide variety of AGN. The torus absorbs the AGN continuum flux and re-emits the reprocessed UV and X-ray photons in the infrared (IR), leading to the observed thermal IR bump (dot-dashed magenta line in Fig. 1.2). The inner rim of the torus corresponds to the sublimation radius, where the dust grains can survive the AGN radiation field (Barvainis 1987), and determines the boundaries of the BLR (e.g. Suganuma et al. 2006).

1.1.2 Variability

Variability is one of the most important characteristics of AGN. The bright and persistent emission, covering the whole magnetic spectrum, is variable over a wide range of timescales, from years to minutes (Ulrich et al. 1997). The detection of rapid variability in the emission from the cores of active galaxies suggested early on that the size of the emitting region is small, no more than a few light days (Greenstein & Schmidt 1964; Terrell 1964). The estimates for the size of the emitting region follow from the causality argument, that states that the light-travel time of the source is of the order of the variability timescale. These estimates favoured the idea that accretion onto a supermassive black hole power the source. Over the years, variability studies have been crucial to the understanding of the underlying physical processes of the emitting region (Mushotzky et al. 1993; Ulrich et al. 1997; Gaskell & Klimek 2003).

While the continuum variability provided estimates on the size of the source, emission-line variability has been a fundamental tool in determining the masses of the black holes in the center of active galaxies (see Peterson 2014, for a review). Variability is thus vital to the understanding of the powering engine of AGN. In the context of this thesis, optical/UV and X-ray variability are particularly important and will be discussed in more detail below.

Optical/UV variability and reverberation mapping

Variations in the optical and UV light curves of AGN are highly correlated (e.g. Cameron et al. 2012), implying that the variability in both bands originates from a common physical region, in particular, the accretion disk which is thought to be responsible for most of the emission at these wavelengths[1]. The timescales for variability in these bands are wide in range, covering timescales of less than one day up to months and years. The origin of the variability has been associated with reprocessing of the X-rays in the disk (e.g. Krolik et al. 1991). This idea is supported by observations of correlated variability between the optical/UV and the X-rays, and associated time lags (e.g. Cameron et al. 2012; McHardy et al. 2014). Nonetheless, it has been found that not all the optical/UV variability can be explained due to X-ray irradiation of the disk by the central source (e.g. Arévalo et al. 2009; Breedt et al. 2010). Longer term variability is hence thought to originate directly from the disk. While obscuration of the ionizing continuum by gas crossing the line of sight may add an additional contribution to the observed variability in AGN (both in the optical/UV and X-rays), it is now widely accepted that most of the observed variability is intrinsic (Padovani et al. 2017).

In addition to the underlying continuum, the broad-emission lines present in the spectra of AGN have also been found to vary. Variations in the flux and profile of the emission lines have been connected to continuum changes, which drive a response in the gas producing the lines. The lines 'reverberate' the continuum emission with a delay due to light travel times within the broad line region. Monitoring the emission-line response to the continuum variations allowed tight constraints to be placed on the geometry of the broad-line region. This method was formally introduced by Blandford & McKee (1982), who first referred to it as *reverberation mapping*. Measuring these time delays yields an estimate of the distance of the clouds to the central source which, combined with the line velocity widths, can be used to infer the mass of the central black hole (for a review see Peterson & Bentz 2006). Nowadays, extensive reverberation mapping campaigns unveil the detailed structure of the broad line region (e.g. Pancoast et al. 2013; Grier et al. 2013), while still being a powerful tool for accurate measurements of black hole masses (e.g. Grier et al. 2012).

[1] This excludes the case of blazars, for which variability in these bands may be dominated by the emission associated with a relativistic jet (Ulrich et al. 1997, for a review).

X-ray variability and time lags

The X-ray light curves of AGN show the most rapid variability. The erratic and (mostly[2]) aperiodic nature of the time series (Lawrence et al. 1987; McHardy 1989) is also characterized by larger amplitude variations occurring on longer timescales. This kind of behaviour can be associated with *red noise* (Press 1978) and can be inferred from the shape of the power-spectral density (PSD). The PSD results from the squared amplitude of the Fourier transform, and it is an important tool to assess the power of the variability at different timescales. Generally the shape of the PSDs is well described by a power-law which decreases steeply at high Fourier frequencies (short timescales), although some sources show more complex power spectra (see e.g. the power-spectral density of NGC 4051 shown in Fig. 1.3), preferring a bending power-law model with flatter power-spectra below a characteristic bending frequency (see González-Martín & Vaughan 2012), which scales linearly with black hole mass (e.g. Uttley et al. 2002; McHardy et al. 2006).

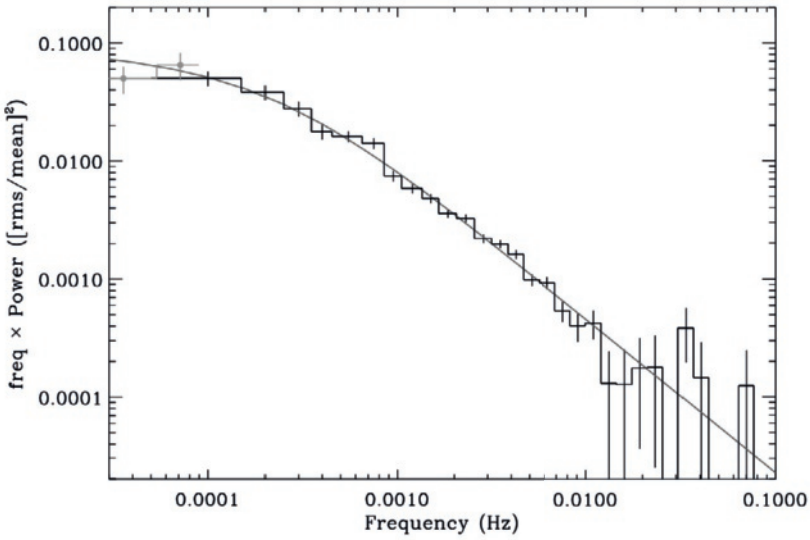

Figure 1.3: Broad-band power spectral density of NGC 4051 obtained from XMM-*Newton* observations ($0.2 - 10$ keV). The solid curve represents the best-fitting bending power-law continuum model. Credit: Vaughan et al. (2011a).

These intrinsic flux variations in the X-ray band are thought to originate from the innermost regions of the accretion flow. An important characteristic of the X-ray vari-

[2]Quasi-periodic oscillations, when they exist, are very difficult to uncover in AGN (Vaughan & Uttley 2005, 2006) and have only been robustly detected in the X-ray time series of the Seyfert galaxy RE J1034+396 (Gierliński et al. 2008; Alston et al. 2014).

ability in AGN, usually referred to as *'rms-flux relation'* (Uttley & McHardy 2001), shows that sources are more variable when brighter. This led to the acknowledgment that the underlying physical processes driving the variability are multiplicative rather than linear, which favours accretion rate variation models as the possible mechanism for the origin of the X-ray variations (Uttley et al. 2005). The origin of X-ray variability is hence explained due to inward-propagating mass accretion fluctuations (Lyubarskii 1997; Arévalo & Uttley 2006), which also ought to be responsible for driving the variability in optical/UV.

The characteristics of AGN variability in the X-rays depend not only on timescale but also on the observed energy band. Different energy bands display different behaviour at different timescales. In particular, the soft X-ray photons have been found to lag the photons in the hard X-ray band on short timescales (see top panel of Fig. 1.4), while at longer timescales the soft emission leads the hard (see bottom panel of Fig. 1.4). Interpreting this complex timescale dependent behaviour in the

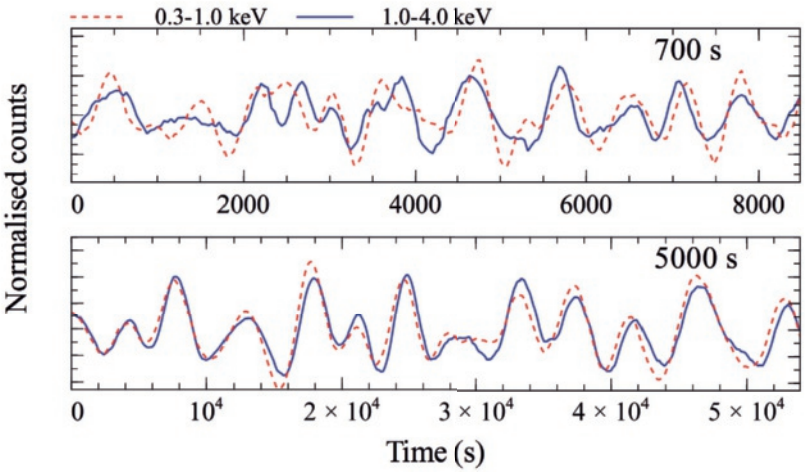

Figure 1.4: Two light curve segments of 1H0707 for the soft ($0.3 - 1.0$ keV, in red) and hard ($1.0 - 4.0$ keV, in blue) X-ray bands, filtered to the timescales of interest. The top panel shows the light curves with a time binning of 700 s showing the soft X-rays lagging the hard band. On the bottom panel, the light curves are presented for a time binning of 5000 s, where the emission from the soft photons leads the variations in the hard X-ray band. Credit: Zoghbi et al. (2010).

time-domain can be quite challenging. The use of Fourier methods[3] is here particu-

[3]The Fourier methods used for the estimation of the spectral-timing products here discussed, such as lag-frequency and lag-energy spectra, can be found in Section 2.4, following the detailed recipes by Uttley et al. (2014).

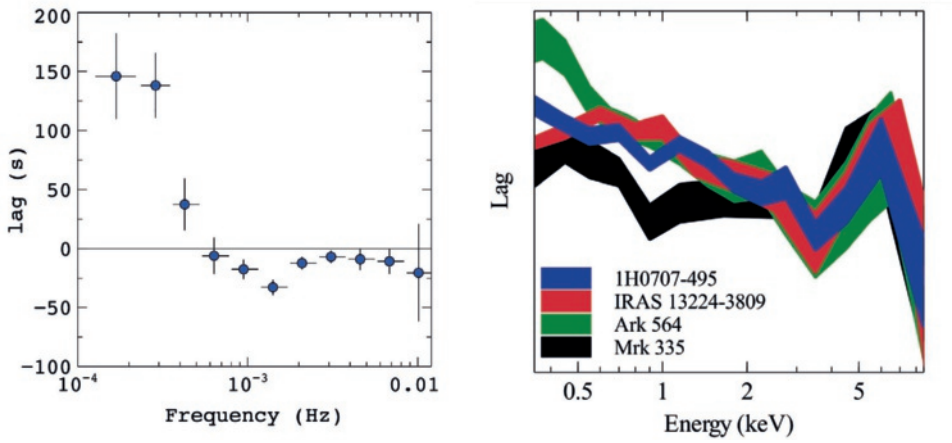

Figure 1.5: Left: Lag-frequency spectrum of 1H0707 for the soft (0.3 − 1.0 keV) vs the hard(1.0 − 4.0 keV) X-ray band. Credit: Zoghbi et al. (2011). Right: Lag-energy profiles for some of the sources that exhibit Fe K lags. The lag-energy spectra are computed by the estimation of the time lags between a narrow energy band and a broad continuum band, over a (Fourier) frequency range of interest. Credit: Kara et al. (2013).

larly convenient, allowing for the different processes associated with the time lags to be disentangled in a straightforward way. The lag-frequency spectrum is a useful tool to illustrate the time-lags between two time series as a function of Fourier-frequency (which corresponds to the inverse of the timescale considered). It is common in AGN to distinguish a dual type of behaviour in the lag-frequency spectrum, which relates to the complex timescale-dependent behaviour mentioned above. At low Fourier frequencies (long timescales) a positive (hard) lag is identified, meaning that the soft photons lead the hard, while at high Fourier frequencies the hard emission leads the soft, resulting in a negative (soft) lag (see left plot in Fig. 1.5). The first robust detection of a high-frequency soft lag in AGN was reported by Fabian et al. (2009), and was associated with reverberation from the irradiated accretion disk. Through an extensive study considering dozens of sources, De Marco et al. (2013) found the amplitude and frequency of the soft lag to be well correlated with black hole mass and suggested the emitting region to be within ten gravitational radii. The discovery of the Fe Kα lags in the lag-energy spectra (Zoghbi et al. 2012; see also Kara

et al. 2016), where the energy dependence of the lags can be appreciated at higher spectral resolution, strongly suggests that this line is a reflection feature (see right plot on Fig. 1.5). The low-frequency hard lags are thought to originate due to inward propagation of fluctuations in the inner accretion flow (Kotov et al. 2001; Arévalo & Uttley 2006) which naturally explains why the outermost soft X-rays respond before the the innermost hard X-rays. It has recently been found (Silva et al. 2016, see chapter 2) that the ionized outflow present in many of the AGN with the aforementioned timing properties is able to introduce a soft lag at low frequencies, resultant from a delayed response of the soft photons (which are more affected by absorption) to variations in the ionizing continuum. The timescales involved in the case study of NGC 4051 are too long to be related to the Fourier frequencies at which reverberation lags are detected, however they may affect the measured hard lags, specifically by diluting them or even producing dominant soft lags at low frequencies (see chapter 2).

Due to their stochastic nature, light curves alone do not yield relevant information on the underlying driving mechanisms. It is through the study of the temporal properties of the variability through the modelling of the observed PSDs and, the lag-frequency and lag-energy spectra, that information on the underlying processes may be uncovered, when time-average spectral models alone are degenerate. Additionally, temporal variability properties must also be taken into account when modelling AGN spectra and consistently explain the timing and spectral properties of the source. Spectral-timing analysis is currently a rapidly developing area of research and of significant importance in the study of AGN.

1.1.3 Outflows & Feedback

A natural consequence of accretion onto the supermassive black hole is the transfer of radiative or kinetic energy to its host galaxy in the form of outflows. Powerful outflows are capable of impacting the surrounding medium by depleting the host galaxy of cold gas, which results in quenching of star formation and hence prevents farther black hole growth (e.g. Di Matteo et al. 2005; Hardcastle et al. 2007; Crenshaw & Kraemer 2012; King & Pounds 2015). In fact, observational evidence indicates that the AGN must somehow be able to regulate the growth and co-evolution of the central supermassive black hole and the host, since the mass of the black hole is found to correlate with both the galaxy bulge mass (e.g. Häring & Rix 2004, and references therein) and the bulge-stellar velocity dispersion, in what is known as the $M_{\rm BH} - \sigma$ relation (Ferrarese & Merritt 2000; Gebhardt et al. 2000, see Kormendy & Ho 2013 for a recent review).

Outflows are commonly observed in AGN, either in the form of highly collimated relativistic jets or less collimated winds of ionized gas. Jets are driven in the near vicinity of the black hole and their structure is usually aligned with the symmetry of the system, perpendicular to the accretion disk plane (see Fig. 1.1). Emission from jets

is mostly dominated by synchrotron radiation, producing a characteristic flat radio spectrum which extends up to IR wavelengths, although inverse Compton scattering of the synchrotron photons may be responsible for additional contribution to high energies, in X-ray and γ-ray bands (see Romero et al. 2017, for a review). Since jets can extend to large scales (up to $\sim$ 1Mpc) it comes as no surprise that the transported kinetic energy can influence the host galaxy, or even the intracluster medium. Ionized winds, on the other hand, are usually detected through the presence of blueshifted absorption lines in AGN spectra. Powerful quasars often show broad absorption line outflows (BALs) while narrow absorption line outflows (NALs) are more commonly observed in Seyfert galaxies. BALs in powerful quasars are predominantly detected in the UV (e.g. Turnshek 1998), with velocities up to $\sim 0.2\ c$, although they have also been identified in the optical (e.g. Hutchings et al. 2002; Aoki et al. 2006; Hall 2007) and the X-rays (Chartas et al. 2003). The NALs in the UV and X-ray spectra of local Seyferts, which are usually referred to as 'warm absorbers', show more moderate outflow velocities from several 100 up to a several 1000 km/s (Crenshaw et al. 1999, 2003a; Costantini 2010). More recently ultra-fast outflows (UFOs), were detected in the X-ray spectra of Seyfert galaxies. UFOs show blueshifted absorption lines of highly ionized species, such as Fe XXV and Fe XXVI, and middle relativistic outflow velocities, up to $v \sim 0.1\ c$ (see Tombesi et al. 2010, and references therein). Outflows with the properties of UFOs may play a significant role for AGN feedback in low-redshift galaxies (King & Pounds 2015), however the detection of such features and detailed assessment of the properties of the winds remain challenging with current instrumentation. Since the majority of AGN does not display major radio jet features, hence is radio-quiet, assessing AGN feedback in its radiative mode through ionized winds is of high importance to the understanding of the connection between the black hole and its host. Roughly 50% of Seyfert galaxies show the presence of a warm absorber. Observations of these bright and nearby objects, in combination with current instrumentation with high-resolution capabilities, such as XMM-*Newton* and *Chandra*, provide the best opportunity for detailed physical studies of AGN winds. This thesis is focused on the spectral and timing properties of warm absorbers and, for this reason, these will be introduced in more detail in the following section.

1.2 Warm absorbers in AGN

1.2.1 History and early observations

First evidence for absorption by ionized material in AGN was reported by Halpern (1984), using X-ray observations of the quasar MR2251-178, taken with the Einstein Observatory. Halpern (1984) detected a large increase in the absorbing column density between observations ~ 1 yr apart and proposed the variability in absorption to be caused by a 'warm absorber', resultant from photoionization of a cloud, or shell of material in the line-of-sight, by the nuclear X-ray radiation. EXOSAT and Ginga observations of NGC 4151 (Yaqoob et al. 1989) and MCG-6-30-15 (Nandra et al. 1990), suggested the presence of X-ray absorbing gas in the spectra of these sources. ROSAT observations revealed the presence of photoelectric edges from ionized ions, confirming the existence of warm absorbers in Seyfert galaxies (e.g. Nandra & Pounds 1992; Fiore et al. 1993; Turner et al. 1993). Early observations with ASCA consolidated these results and allowed for the first constraints on the ionization state of the gas due to the sensitivity and resolution of its detectors. Comparison to photoionized models (Kriss et al. 1996) and variability of the absorption edges (Reynolds et al. 1995; Otani et al. 1996) led to the conclusion that more than one absorbing component were at play, suggesting a more complex structure of the warm absorber. Sample studies of the numerous observations from ASCA confirmed that at least 50% of Seyfert galaxies show the presence of a warm absorber (Reynolds 1997; George et al. 1998).

The launch of the *Chandra* and XMM-*Newton* observatories revolutionized the study of X-ray ionized absorbers. Equipped with high spectral resolution grating spectrometers and collecting high signal-to-noise data, these two satellites have been responsible for great advances in the field. From the first observations, a rich absorption line spectrum of C, N, O, and Fe-L transitions could be unveiled in the soft X-rays (Kaastra et al. 2000; Kaspi et al. 2000). The narrow absorption lines were observed to be blueshifted relative to the systemic receding velocity of the galaxy, indicating that the gas was in fact outflowing.

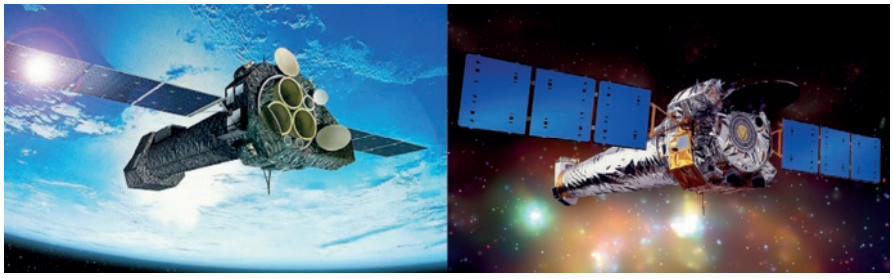

Figure 1.6: Left: Illustration the X-ray space observatory XMM-*Newton*. Image credit: ESA. Right: Illustration of the *Chandra* X-ray observatory. Image credit: NASA.

1.2.2 Modelling the ionized absorber

Photoionization is a bound-free process and occurs when an electron is removed from an ion due to energy transfer from an the incident photon. In AGN, the absorbing outflowing gas is exposed to the strong radiation field from the central source and therefore photoionization primarily governs the physical conditions of the gas.

Photoionization models

Constraining the properties of the gas is thus possible through photoinization models[4]. Models generally assume an infinite (in the plane perpendicular to the incident photons) slab of gas, of constant density, irradiated by the ionizing flux, and in photoionization equilibrium. The ionization balance of the gas is then calculated based on the source's SED and assumed elemental abundances (typically solar). This yields the equilibrium ionic column densities and temperature of the gas as a function of ionization, as well as the total hydrogen column density, $N_{\rm H}$ of the slab. The ionization state can be defined by the parameter ξ, which directly relates the ionization of the gas to the ionizing luminosity $L_{\rm ion}$ (defined between 1-1000 Ryd, where 1 Ryd corresponds to 13.6 eV), the gas density, n, and the distance of the gas to the central source, r,

$$\xi = \frac{L_{\rm ion}}{nr^2}. \tag{1.1}$$

The determination of the ionization and thermal structure of the gas with the aforementioned codes make it possible to infer the properties of the gas through spectral fitting.

Spectral fitting

In the UV, the ionic column densities of individual kinematic components can be modeled due to the high spectral resolution available. To find a best fit, the ionization parameter and column density are varied until the predicted ionic columns match the estimated columns from the measured depths of the observed absorption lines.

The lack of sufficient spectral resolution in the X-rays prevents the individual kinematic components from being identified. While the Cosmic Origins Spectrograph on the Hubble Space Telescope has a resolving power of $\mathrm{R} \approx 1550 - 24000$, *Chandra* and XMM-*Newton* have resolving powers of $\mathrm{R} \approx 200 - 1000$. However, in the X-rays, we have access to a rich absorption spectrum populated by numerous transitions of Fe, Si, Mg, C, N and O (see e.g. the RGS spectrum of NGC 3516 in Fig. 1.7), which

[4]Codes commonly used in the field for the modelling of photoionized plasmas are Cloudy (see Ferland et al. 2017, for the latest release), XSTAR (Kallman & Bautista 2001), and TITAN (Dumont et al. 2000). Throughout this thesis I primarily use Cloudy.

allow us to more accurately constrain the ionization state and total column density of the gas. Minimization procedures can then be used to fit the soft X-ray AGN spectra by searching through a grid of ionization parameters and column densities, similarly to what is done for the UV case.

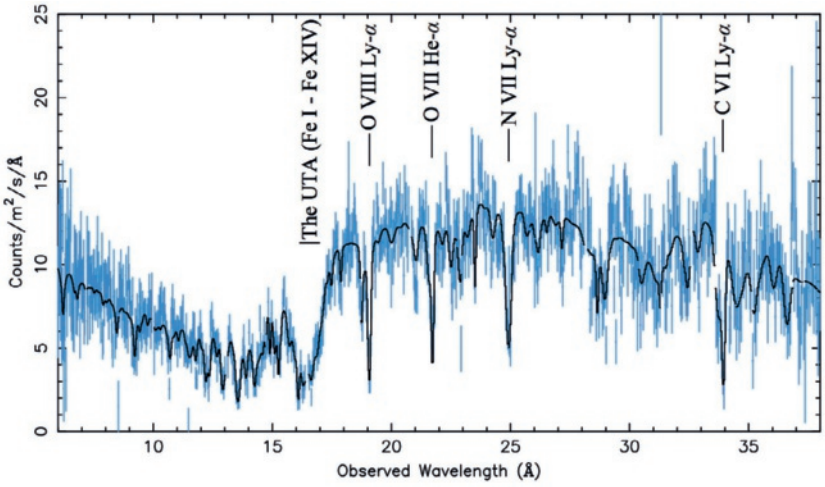

Figure 1.7: RGS spectrum of NGC 3516. Some of the strongest absorption features are labelled. Credit: Mehdipour et al. (2010).

In this thesis we routinely make use of the absorption model XABS (Steenbrugge et al. 2003) included in the spectral fitting package SPEX (Kaastra et al. 1996). The XABS model calculates the transmission spectrum of a slab of photoionized gas, where all the ionic column densities are consistently linked through a previously calculated photoionization model, based on the SED specific for the source, which establishes the ionization balance of the gas. The model takes into account all the relevant ions, even if these are weak absorption features, since the combined effect of all transitions allows for a more accurate solution.

Combined with an appropriate modeling of the underlying continuum, the XABS model yields an estimate of the physical parameters of the gas. The directly constrained warm absorber parameters through spectral fitting are the ionization state, the hydrogen column density, the outflow velocity and the velocity broadening; the latter two are not as tightly constrained as the former due to the reduced resolution capabilities of the X-ray detectors.

1.2.3 Variability and time-dependent photoionization

AGN are variable sources (see Section 1.1.2). The underlying ionizing continuum can vary by more than a order of magnitude, on timescales as short as a few hours. The warm absorbing gas is subjected to these flux variations, becoming more ionized when the flux increases and recombining when the flux decreases. The response of the warm absorber to a variable central source naturally introduces a time-dependent effect on the physical behaviour of the gas.

Primarily, the heating and cooling of the absorbing gas are dominated by photoionization and radiative recombination. As such, the effects induced by the source's variability on the behaviour of gas can be described by the time-dependent ionization balance equations, introduced by Krolik & Kriss (1995)[5]. Consider the relative density n_{X^i} of ion i of a certain species X. Its time-dependent evolution is a function of the electron density of the gas n_{e}, the recombination rate from stage $i+1$ to i (given by the recombination coefficient, $\alpha_{\mathrm{rec\ X}^i}$, times the electron density of the gas), and the ionization rate from stage i to $i+1$, I_{X^i},

$$\frac{\mathrm{d}n_{\mathrm{X}^i}}{\mathrm{d}t} = -n_{\mathrm{X}^i} n_{\mathrm{e}} \alpha_{\mathrm{rec,X}^{i-1}} - n_{\mathrm{X}^i} I_{\mathrm{X}^i} + n_{\mathrm{X}^{i+1}} n_{\mathrm{e}} \alpha_{\mathrm{rec,X}^i} + n_{\mathrm{X}^{i-1}} I_{\mathrm{X}^{i-1}} \tag{1.2}$$

The solutions of this system of N-coupled differential equations define the response time, i.e. the time necessary for the gas to reach equilibrium with the ionizing continuum. In an equilibrium situation, the creation and destruction rates are balanced for each species, yielding $\mathrm{d}n_{\mathrm{X}^i}/\mathrm{d}t = 0$, for all ions. The time-dependent behaviour of the gas is however rarely that simple. A dependence on the history flux of the source may lead the gas to manifest a delayed and smoothed response to the continuum variations or even to appear uncorrelated with the ionizing luminosity, for instance if the gas becomes over-ionized due to rapid and high-amplitude flux variations.

Time-dependent effects are yet not throughly implemented in models of photoionized gas. Nicastro et al. (1999) attempted to study the effects on the ionization state of the warm absorber due to a time-varying ionizing continuum. The results found by Nicastro et al. (1999) have several implications. Firstly, the response, or equilibrium, timescale is inversely proportional to the density of the gas, even in periods of increasing flux, although the recombination timescale is generally much longer than the ionization timescale. Lower densities hence imply longer response times. Additionally the equilibrium abundances of different ions are reached over different timescales adding an extra level of complexity to the time-dependent effects on photoionization. Studying the variability of the warm absorber thus yields an estimate of the density of the gas (e.g. Nicastro et al. 1999; Kaastra et al. 2012; Arav et al. 2012), which in turn allows for an estimate of its distance to the central source (see equation 1.1),

[5]The normally small effects from Auger ionization, collisional ionization, and three-body recombination are neglected in the balance equations described here.

providing crucial information to the understanding of the nature of the gas and its impact on the surrounding environment.

1.2.4 Observational properties and physical constraints

Extensive X-ray observations over the past several years allowed many properties of these outflows to be uncovered (see Crenshaw et al. 2003a, for a review). The understanding of these properties can be gained through the analysis of UV and X-ray data, both by studying the energy spectra and the time variability (see sections 1.2.2 and 1.2.3). The constraints resultant from the observations can then be used to derive a physical model of the absorbing gas and assess its potential effects on the surrounding environment.

Global properties of the gas can be derived from a proper modeling of the observed spectral features, and their overall characteristics can be summarized as follows (see also McKernan et al. 2007). The gas ionization parameter spans over almost four orders of magnitude $\xi \sim 10^0 - 10^4$ erg cm s^{-1}, and often multiple ionization phases are required for a single kinematic component (see e.g. Steenbrugge et al. 2005). The estimated outflow velocities range between a few 100 up to a few 1000 km s^{-1}, with several kinematic components being detected in some sources (see e.g. Pounds & King 2013). Finally, column densities of such absorbers are typically amid $10^{20}-10^{23}$ cm^{-2}.

The fraction of the continuum that is covered by the warm absorber averaged over all lines of sight defines its global covering factor, $C_{\rm g}$. Global covering factors are hard to determine. Observations reveal that at least half of radio-quiet AGN show the presence of a warm absorber. This can lead to two distinct hypotheses regarding the global covering factor of the gas (Crenshaw et al. 2003a). Either $C_{\rm g} \sim 0.5$ for all observed sources, such that for fifty percent of those the gas is out of our line of sight, or $C_{\rm g} \sim 1$ for half of them with the absorbing gas being absent in the remaining 50 per cent. In any case, this implies large solid angles for the X-ray gas. These considerations have important implications for the mass outflow rate of the warm absorber. The covering factor in our-line of sight is also an important property of the gas, as it characterizes the clumpiness of the flow. Discriminating between a homogeneous or clumpy outflow can provide insights on the origin and nature of the absorbing region.

Density and location of the absorber

Other crucial parameters for the assessment of the origin and nature of warm absorbers are the gas density and its radial location. The product of the density and the distance squared is trivial to obtain via the ionization parameter (see equation 1.1). Therefore, constraining the gas density directly yields its distance to the central

source.

The density can be estimated by making use of density-sensitive absorption lines from meta-stable levels. This method, while quite successful in the UV, is very hard to apply in the X-rays (e.g. Kaastra et al. 2004). A different way to derive the density is by studying the variability of the gas. In section (see 1.2.3), I first introduced the concept of variability in warm absorbers. The bottom line here is that the variability of the ionizing continuum induces a response in the gas, which becomes more ionized during periods of increasing flux and recombines when the flux drops. Changes in ionization can be tracked through by monitoring the variations in the absorption lines. If their response time to changes in the continuum can be measured, the density of the gas is obtained. Absorption variability studies are often attempted through time resolved spectroscopy. However, the signal-to-noise ratio is in that case a limitation for short timescales. Detail monitoring of the variations in the gas through time-dependent photoionization is thus more advantageous. The predicted behaviour of the ions, for different densities, can next be used to simulate spectra which are then compared to real data (e.g. Kaastra et al. 2012).

Constraining the density, and hence distance, of warm absorbers remains one of the biggest challenges in the field. The degeneracy of these two quantities and the uncertainties on their estimations have led warm absorbers to be placed at a variety of distances (Crenshaw et al. 2003a), from the host galaxy halo ($\sim$10 kpc), to the inner galactic disk (0.1-1 kpc),the NLR (10-500 pc), the dusty torus ($\sim$ 1 pc), and the BLR (0.01-1 pc).

The X-ray and UV connection

Blueshifted narrow absorption lines are also found in the UV spectra of AGN. In fact, sources with intrinsic UV absorption also show the presence of a X-ray warm absorber (Crenshaw et al. 1999; Kriss et al. 2002), suggesting that both phenomena are related. For this end, simultaneous UV/X-ray observations are essential. However, even in the presence of multiwavelenght campaigns, determining if the observed absorption features arise from the same gas is not trivial (see Costantini 2010, for a review). In the UV, instrumental capabilities allow the individual features in the spectra to be distinguished, which results in accurate kinematic diagnostics of the gas components. In contrast, the ionization state and total column density are hard to constrain due to the nature of the UV gas which shows relatively few ions. The X-ray band, on the other hand, exhibits a rich absorption spectrum populated by numerous atomic transitions, which allow us to constrain the ionization state and column density of the gas, even when the spectral resolution is not ideal to isolate kinematic components. Matching the different absorbing phases detected in the UV to those found in the X-rays is for that reason still a challenge. Nonetheless, evidence for a connection of the absorbing gas has mounted over the last years as a result of dedicated UV/X-ray

campaigns (e.g. Gabel et al. 2005; Costantini et al. 2007b; Ebrero et al. 2011, 2013; Arav et al. 2015). Some of the low ionization components detected in the X-rays are likely to originate from the same gas producing the observed higher ionization troughs in the UV (e.g. C IV, N V).

Origin and driving mechanisms

Outflows can be driven by several mechanisms. In AGN, thermal, radiation pressure, or magnetic driving are all plausible candidates to launch a wind, and one mechanism alone may not be sufficient to explain all AGN outflows (see Proga 2007, for a review). Theoretically it is not trivial to develop models that can easily be tested against available data, making it difficult to predict which mechanism(s) may be dominating. Observationally, the location and geometry of the warm absorbers are hard to constrain and thus their nature is still up for debate.

Derived warm absorber distances often point to a location consistent with the dusty torus (Blustin et al. 2005; Costantini 2010; Sanfrutos et al. 2016). Krolik & Kriss (2001) showed that such an outflow could be produced as a result of photoionized evaporation of the inner parts of the torus. Radiatively driven disk winds are also often evoked (e.g. Murray & Chiang 1995). As modeled by Murray & Chiang (1995), the wind is a continuous flow, originating over a range of disk radii. An observed anti-correlation of the soft X-ray luminosity with the width of the C IV UV absorption line (Proga et al. 2000), as well as the presence of line-locking in the spectra of broad absorption line quasars (Foltz et al. 1987; Weymann et al. 1991; Korista et al. 1993; Arav et al. 1995; Arav 1996), support this launching mechanism. Furthermore, Arav et al. (2005) found the shape of the absorption lines to be asymmetric, consistent with what is predicted by line driven radiation pressure codes.

The recently discovered UFOs (see Sec. 1.1.3), are likely to originate in the inner accretion disk (Tombesi et al. 2012) and possibly driven via Magneto-Hydrodynamic processes (Kraemer et al. 2017). However, a possible connection of these highly ionized, high velocity outflows to the classical warm absorbers is still a matter of ongoing research.

AGN feedback

Considering that radio-quiet sources can be up to 90% of all AGN, and that at least half of these may show a warm absorber, it is crucial to understand how the outflows interact with their surroundings.

The mass outflow rate, $\dot{M}_{\rm out}$, can be estimated via the observable parameters

discussed above as given by Crenshaw & Kraemer (2007):

$$\dot{M}_{\rm out} = 4\pi r N_{\rm H} m_{\rm p} C_{\rm g} v, \tag{1.3}$$

where r is the distance of the gas to the central source, $N_{\rm H}$ is the column density of the gas, $m_{\rm p}$ is the proton mass, $C_{\rm g}$ the global covering factor and v the outflow velocity. The kinetic energy of the flow, which is dependent both on the outflow velocity and the mass outflow rate, can then estimated, and is given by

$$L_{\rm kin} = \frac{1}{2}\dot{M}_{\rm out} v^2 \text{erg s}^{-1} \tag{1.4}$$

The mass outflow rates can be comparable to the mass accretion rates or higher (Crenshaw & Kraemer 2007), though the mechanical power of the flow is merely on the order of 0.1% of the bolometric luminosity (Costantini 2010), suggesting that the warm absorber has a modest impact for feedback. Nonetheless, these results are limited by the uncertainties on the estimated values for the radial distance and covering factor of the flow, which are often only loosely constrained. Equations 1.3 and 1.4 show that the impact of the outflows has a dependence on the outflow velocity of v^3. In light of this, the higher velocity UFOs have a wider potential for non-negligible contribution to AGN feedback (King & Pounds 2015). Additionally, large distance outflows (Arav et al. 2008; Di Gesu et al. 2013) are potentially capable of also contributing to feedback.

1.3 Future prospects

Since being first observed in the 80s, our understanding of ionized outflows has grown remarkably. Instrumental capabilities have played a major role in the assessment of the physical properties of the gas over the past decades. Despite the great discoveries which were only made possible with the advent of *Chandra* and XMM-*Newton*, there are yet fundamental questions to be answered. Are the different ionized absorbers (UV, soft X-rays, UFOs) intrinsically part of the same outflow? What are the driving mechanisms of the gas and where do they originate? Can ionized outflows have an important contribution to AGN feedback?

For the next few years X-ray astronomy will remain dependent on the currently flying observatories. XMM-*Newton* is expected to operate for another decade, granting the opportunity for comprehensive campaigns dedicated to AGN monitoring. Deep observations of known sources, combined with multi-wavelength coverage, prove to still be relevant to advance current knowledge of AGN. Probing the short and long-timescale variability can in turn be used to, for instance, infer the distance of the warm absorber to the source (e.g. Kaastra et al. 2012), or to reveal the dynamical structure of the corona through reverberation studies (Fabian et al. 2017).

In the long term, a major breakthrough in X-ray astronomy is expected with the next generation of X-ray observatories. Below, I describe some of the highlights of the most exciting future X-ray missions.

1.3.1 X-ray Astronomy Recovery Mission (XARM)

Following a successful launch in February 2016, the JAXA/NASA X-ray collaboration satellite Hitomi was unexpectedly lost shortly after. Hitomi carried a variety of instruments, of which SXS, a high resolution calorimeter, was the most relevant to advance spectroscopic studies in the X-rays. Despite the incident, Hitomi was still able to observe its first target, the Perseus cluster, and exceeded expectations. These observations resulted in numerous publications, with the major results being reported in Nature by the Hitomi Collaboration (2016). Following the loss of Hitomi and based on the outstanding performance of SXS, joint efforts from JAXA, NASA, and ESA, resulted in the approval of a recovery mission, XARM, which is expected to launch in 2021. Instruments on board XARM will be a soft X-ray calorimeter spectrometer and a soft X-ray imager, both having similar characteristics to the SXS and SXI instruments developed for Hitomi. The sensitivity of the soft X-ray calorimeter grants a spectral resolution of 5 eV in the energy range of 0.5 - 12 keV which, as demonstrated by the first observations from Hitomi, will revolutionize many scientific areas of X-ray astronomy, including the study of ionized outflows. In particular, detailed studies of ionized absorption at higher energies will be possible for the first time (see Fig. 1.8; and see Kaastra et al. 2014b, for details). This will allow for a more reliable characterization of UFOs, which due to their high outflow velocities are supposed to play an important role on AGN feedback (King & Pounds 2015).

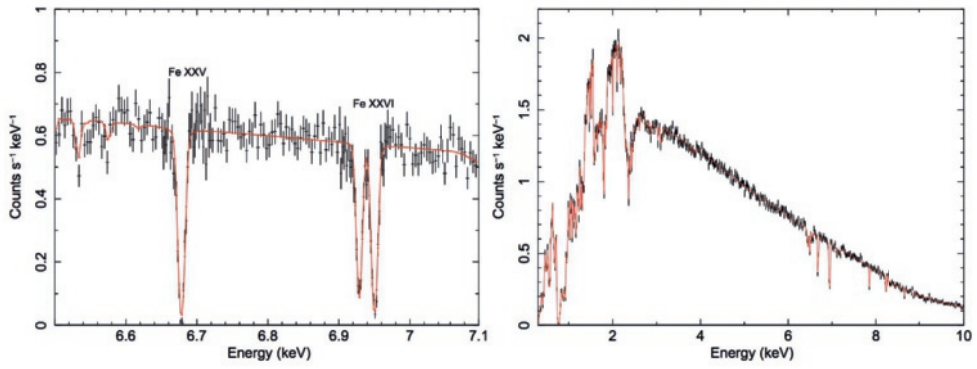

Figure 1.8: Simulated spectrum for NGC 4151, for 100 ks exposure time with SXS. Credit: Kaastra et al. (2014b).

1.3.2 Athena

Athena is an European Space Agency (ESA) X-ray mission, expected to launch in 2028 and will provide a giant leap on the understanding of the hot an energetic universe (Nandra et al. 2013). The most superb capabilities of Athena are based on its effective area, which largely exceeds previous missions (see left panel of Fig. 1.9), while retaining a spectral resolution of 2.5 eV over a broad X-ray band (0.3-10 keV). Regarding AGN studies, Athena will provide exceptional new science. From a spectral point of view, the high sensitivity over a large X-ray energy band, will allow a detailed characterization of most of the ionization states present in the absorbing gas providing essential information to the understanding of AGN outflows (Cappi et al. 2013).

At the same time, the large effective area permits the study of variability in greater detail, not only through time-resolved spectroscopy, but most importantly through spectral timing techniques. X-ray reverberation is a novel tool to map the innermost regions of AGN and while much progress has been achieved over the past years with XMM-*Newton*, this method will highly profit from the exquisite quality data offered by Athena. With Athena the time lag spectrum can be obtained at much higher resolution (see right panel of Fig. 1.9) over a broader frequency range, probing new timescales and granting the possibility to de-couple the different emission mechanisms (Dovciak et al. 2013).

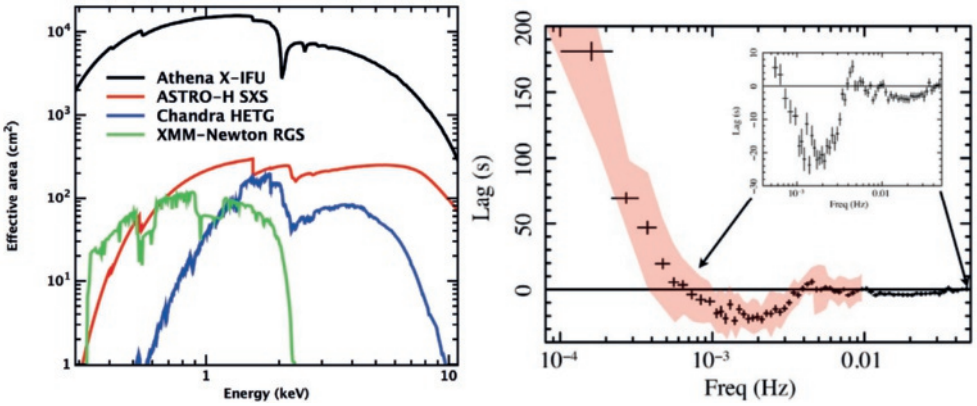

Figure 1.9: Left: Athena performance in terms of effective area for high-resolution spectroscopy compared to earlier missions. Credit: Barcons et al. (2015).; Right: Expected time lag spectrum (0.3-1 keV vs 1-4 keV) with Athena for 1H0707-495 (exposure time as in the XMM-*Newton* observation, i.e. 500 ks). The red region is the 1σ contour with XMM-*Newton*. Credit: Dovciak et al. (2013).

1.3.3 Arcus

Arcus is a high resolution X-ray grating spectrometer mission that was proposed to NASA and is currently under study (Smith et al. 2016). If approved, Arcus is expected to launch in 2023 and its resolution in the soft X-ray band will be $\sim$ one order of magnitude higher than XMM-*Newton*, *Chandra*, XARM, or even Athena. Due to its increased sensitivity, Arcus would be capable of detecting lower column density absorbers and resolving the absorption features into all their kinematic components (see Fig. 1.10), similarly to what is achieved nowadays with UV data, and the possibility of density-diagnostics with metastable levels would become a reality in the X-rays (Kaastra 2017a). Consequently, AGN feedback studies would highly benefit from the mission.

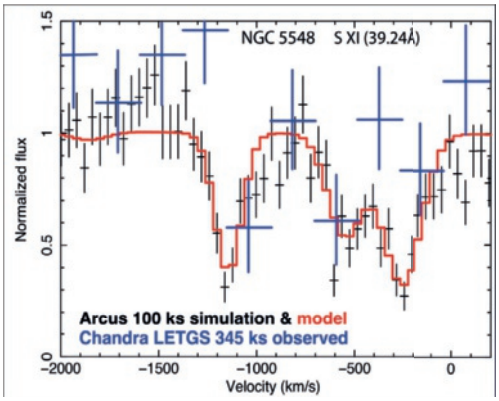

Figure 1.10: *Chandra* LETGS spectrum of NGC 5548 around the S XI line, with an exposure time of 345 ks, and a 100 ks simulation of the same spectrum with Arcus. The solid line indicates the model used for the simulation (see Kaastra et al. 2014a, for details). Credit: Figure publicly available at www.arcusxray.org, adapted from Kaastra (2017a).

1.4 Thesis outline

This thesis focus on the study of ionized outflows in AGN. The study of these outflows is of extreme importance to understand the real impact they have in the surroundings of the AGN, which has not been quantified yet. The studies presented and techniques developed here, aim to uncover the spectral and temporal properties of the ionized gas and set the path for future missions, which will allow these methods to be routinely used for mapping AGN outflows in great detail. In Chapter 2, I present a novel technique to study the response time of the ionized gas to changes in the continuum by looking for signatures of this possible extra time delay in the X-ray time lags of NGC 4051. This technique involves a combination of spectral-timing analysis and

time-dependent photoionization modeling. Applying this method to the extensive XMM-*Newton* observations of NGC 4051, I show that the warm absorber in this source is capable of producing a soft lag (up to 100 s) at low Fourier frequencies, due to the response time of the gas to variations in the flux of the ionizing source, as a result of photoionization and radiative recombination. This study shows for the first time the effects of photoionized absorption on the X-ray time lags of AGN and explores the use of spectral-timing analysis to characterize the outflow. In Chapter 3, I expand the time-dependent photoionization model developed in the work of Chapter 2 and apply it to the study of ionized absorbers in the UV. Using this model, I predict the variations in the ionic column densities of the absorbing gas, as it reacts to the variability of the central source, for a grid of gas densities and ionization parameters. In the optically thin limit, the ionic column densities are directly proportional to the equivalent widths of the absorption troughs. This linearity allows for a direct comparison of the model predictions with the measured equivalent width light curves. By fitting the time-dependent models to the exquisite data obtained for NGC 5548, taken with the Cosmic Origins Spectrograph on HST, I am able to constrain both the density and the ionization state of the gas. These results highlight the potential of time-dependent photoionization models to retrieve key physical parameters of the gas. Finally, in Chapter 4 I analyse in detail new X-ray observations of the Seyfert 1 galaxy I Zwicky 1, focusing on the rich soft X-ray absorption spectrum. The variability of the absorber in this source does not show a correlation with the ionizing source, in contrast to what is expected from classical photoionization models. The changes in ionization and column density of the gas over the years point instead to a non-homogenous outflow, where different clumps of different densities cross the observer's line-of-sight over the years. The temporal behaviour of the gas in this source is not easily explained by classical scenarios, substantiating the need for theoretical models capable of reproducing more complex variability.